Adsorption (2007) 13: 281–290
DOI 10.1007/s10450-007-9027-3

Synthesis of SBA-15/carbon composite with an ink-bottle-like pore structure by a novel pulse CVD technique

Chun He · Frank L.Y. Lam · Xijun Hu

Received: 28 April 2007 / Revised: 13 July 2007 / Accepted: 16 July 2007 / Published online: 20 September 2007

Abstract A novel and easy post modification method, pulse chemical vapor deposition (pulse CVD), was developed to tailor the pore-opening of SBA-15 while largely keeping its surface area and pore volume. By using acetylene as carbon precursor and nitrogen as carrier gas, the pore-mouth of SBA-15 was effectively reduced from 8.1 nm to 5.1 nm within 5 min while maintaining the pore body at 8.1 nm. This ink-bottle-structured SBA-15/carbon composite only losses 12% BET specific surface area and 16% total pore volume, respectively. The SBA-15/carbon composite is highly hexagonally ordered and has similar particle morphology as the original SBA-15. The effect of three pore modification factors—the number of cycles of pulse CVD, the ratio of acetylene/nitrogen and the feeding time of carbon precursor, on the final pore structure of the SBA-15/carbon composite is also studied.

Keywords SBA-15 · Pulse CVD · Ink-bottle-like pore

1 Introduction

During last decades, highly ordered mesoporous SBA-15 silica has attracted much attention and has been modified and applied in the fields of catalysis, separation, water purification, and advanced optics devices (Shin et al. 2001; Kruk et al. 2003). This remarkable interest stems from the many desirable features of SBA-15, including well-defined hexagonal structure, high surface area, narrow mesopore size distribution, large pore volume, large tailorable pore size, high degree of structural ordering, high thermal/hydrothermal stability, ease of synthesis, availability of economically facile synthesis pathways, etc. (Zhao et al. 1998a, 1998b; Shin et al. 2001; Kruk et al. 2003). SBA-15 silica, however, like other mesoporous silica, has relatively lower adsorption capacity than microporous adsorbents in the low concentration region and is more hydrophilic than carbon surface.

Narrowing the pore-opening size of microporous and mesoporous materials has been a very interesting field for many researchers in recent years in order to improve the adsorbent's shape or size selectivity and/or adsorption capacity. The deposition of thin silica layers on zeolites by chemical vapor deposition (CVD) (Hibino et al. 1991; Kunkeler et al. 1997; Begum et al. 2001) or chemical liquid deposition (CLD) (Weber et al. 1998, 2000; Zheng et al. 2002) from tetraalkyl orthosilicates, e.g. tetraethoxysilane (TEOS) and tetramethoxysilane (TMOS), or chemical liquid deposition (CLD) from metal halides such as $SiCl_4$, $TiCl_4$ and $SbCl_5$ (Yue et al. 1996, 1997), has been employed as a pore-size engineering technique to improve the shape selective properties by passivation of the external surface acidity (blocking non-shape-selective active sites for secondary reactions) and/or by narrowing the pore entrances (enlarging differences in the diffusivities of isomers).

CVD of tetramethyl orthosilicate (TMOS) and tetraethyl orthosilicate (TEOS) has also been studied to narrow the pore mouth of mesoporous MCM-41 (Zhao et al. 1999; Hu et al. 2001; Fodor et al. 2002; Mehn et al. 2002) in order to improve its adsorption capacity in the low concentration region. Zhao and coworkers (Zhao 1998; Zhao et al. 1999; Hu et al. 2001) put forward a novel tailoring procedure to tune the pore-opening of MCM-41 from ∼ 3 nm to 1.4 nm without influencing the diameter along the whole length of

C. He · F.L.Y. Lam · X. Hu (✉)
Department of Chemical Engineering, Hong Kong University of Science and Technology, Clear Water Bay, Kowloon, Hong Kong
e-mail: kexhu@ust.hk

the tubes. The modified MCM-41 exhibits a type I adsorption isotherm for nitrogen and benzene, and its adsorption performance for low-concentration volatile organic compounds (VOCs) has been significantly improved.

Efforts on pore structure alteration of porous carbon to generate pore constriction leading to sieving properties have also been performed by various research groups. In the pore narrowing technique, cracking of hydrocarbon is usually employed to facilitate the deposition of carbon over the pore mouth of the micropore. Carbon deposition from the gas phase on solid substrates by total decomposition of hydrocarbons played a highly undesirable role in petrochemistry from the very first (Benzinger et al. 1996). On the other hand, decomposition of volatile hydrocarbons at high temperature is used to deposit carbon in a well-defined manner as a so-called pyrolytic carbon or pyrocarbon on or in substrates. Microporous carbon molecular sieves have been successfully synthesized by CVD of volatile hydrocarbon or catalytic coke deposition (Kawabuchi et al. 1996, 1997; Prasetyo and Do 1999; Freitas and Figueiredo 2001; de la Casa-Lillo et al. 2002; Villar-Rodil et al. 2002, 2003, 2005; Paredes et al. 2003; David et al. 2004; Carrott et al. 2006) on microporous carbon materials.

In this research, a novel and easy post modification method, carbon pulse chemical vapor deposition (carbon pulse CVD), was developed to tailor the pore-opening of meosporous SBA-15 silica aimed at synthesizing a SBA-15/carbon composite with an ink-bottle-like pore structure. The effect of three factors: the number of cycles of CVD, the ratio of acetylene/nitrogen and the feeding time of carbon precursor, on the final pore structure of the modified SBA-15 was discussed. The influence of the carbon deposition on the particle morphology and periodic pore structure was also investigated.

2 Experimental

2.1 Preparation of SBA-15 silica

Pure silica SBA-15 samples were synthesized using triblock copolymer, $EO_{20}PO_{70}EO_{20}$ (Pluronic P123, Aldrich), as the template and tetraethylorthosilicate (TEOS, 98%, Aldrich) as the silica source, following the synthesis procedure reported by Choi et al. (2003). Basically, P123 was dissolved in hydrochloride solution at 308 K. After that, TEOS was added under stirring to the above mixture. The molar composition of the final gel was: 1 TEOS:0.017 P123:0.54 HCl:99.5 H_2O. The resulting gel was then transferred into a Teflon-lined stainless steel autoclave, heated to 373 K and kept at that temperature for 24 hours. The final product was filtrated without washing, dried at 333 K overnight and calcined at 823 K for 12 hours to remove the template.

2.2 Synthesis of SBA-15/carbon composite with an ink-bottle-like pore structure

The SBA-15/carbon composite with an ink-bottle-like pore structure was synthesized at 1073 K using acetylene as the carbon precursor, nitrogen as the carrier gas and SBA-15 as the substrate in the home-made pulse CVD system as schematically shown in Fig. 1.

Typically, prior to carbon pulse CVD experiment, 0.2 g substrate SBA-15 was loaded in a quartz reactor and subsequently evacuated to vacuum. The substrate was then heated to 573 K and kept at that temperature for 3 hours under vacuum with the flowing of nitrogen (60 cm^3/min) to remove any moisture and impurities. After finishing the outgassing process, the substrate was heated to 1073 K under flowing of nitrogen (60 cm^3/min). Then, acetylene (12 cm^3/min) was fed with nitrogen (48 cm^3/min) into the reactor for 5 min. After that, the reactor was purged with nitrogen at the operating temperature for 15 min to remove unreacted feed and volatile products before cooling down to room temperature (or next injection of the carbon precursor in the case of more cycles of pulse CVD experiment). The resulting material possesses an ink-bottle-like pore geometry as illustrated in Fig. 2.

During each experimental run, the flow rates of acetylene and nitrogen were separately controlled by two mass flow controllers. Blank experiment was also performed by treating the same amount of SBA-15 sample in the same way without feeding acetylene. In addition, during the whole reaction process, the quartz reactor was kept rotating in order to achieve uniform deposition of carbon on the substrate.

2.3 Characterization

2.3.1 Nitrogen adsorption

Nitrogen adsorption/desorption isotherms were performed on a Quantachrome Autosorb 1 at liquid nitrogen temperature. Before the adsorption measurements, samples were outgassed at 573 K overnight. The BET specific surface area was calculated from nitrogen adsorption data in the relative pressure range from 0.05 to 0.2. The total pore volume was estimated from the amount of nitrogen adsorbed at a relative pressure of about 0.99. Pore size distribution was calculated using the non-local density functional theory (NLDFT) method. The kernel of NLDFT equilibrium capillary condensation isotherms of nitrogen at 77 K on silica was selected for the model isotherms. Micropore volume was calculated from t-plot method using nitrogen adsorption data below relative pressure of 0.4.

2.3.2 X-Ray Diffraction (XRD)

X-ray diffraction patterns of samples were recorded on a PANalytical X'pert Pro powder X-ray diffractometer

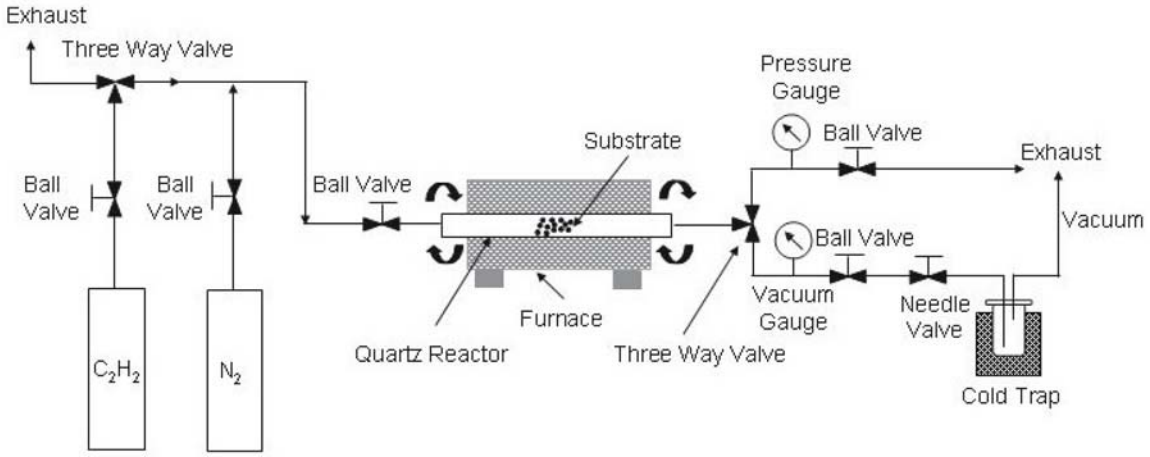

Fig. 1 Schematic diagram of carbon pulse CVD setup

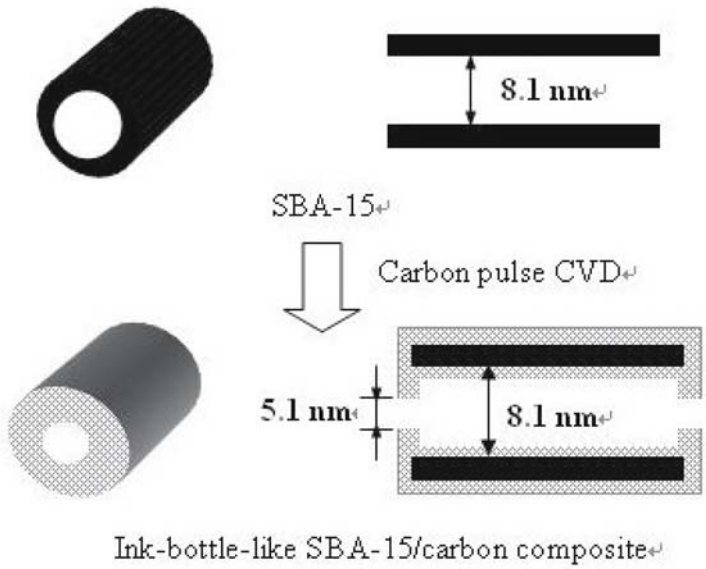

Fig. 2 Schematic model for tailoring the pore-opening size of SBA-15

equipped with Cu anode. Samples were scanned from 0.5 to 3 degrees 2θ in steps of 0.05 degree 2θ per second with a count time of 5 seconds at each point.

2.3.3 Thermogravimetric Analysis (TGA)

Weight change profiles and derivative weight change curves of samples were measured on a thermogravimetric analyzer (Perkin Elmer TGA 7) from room temperature to 1073 K with a heating rate of 10 K per min in air.

2.3.4 Scanning Electron Microscopy (SEM)

Samples were mounted on a sample plate with an adhesive double-side carbon tape and coated with gold to increase the electronic conductivity. The particle morphologies were observed on a JEOL JSM 6300F ultra-high resolution scanning electron microscope with a cold field emission gun.

2.3.5 Transmission Electron Microscopy (TEM)

Samples were suspended in ethanol (99.9%) by ultrasonication and deposited on a carbon coated copper microgrid. The imaging was performed at a room temperature using a JEOL 2010 TEM.

3 Results and discussion

The CVD of carbon involves simultaneous processes of complex gas-phase reactions, such as molecular and free radical chain reactions, simultaneous decomposition and polymerisation, as well as phase change from gas to liquid or solid, leading to various products including polycyclic aromatic hydrocarbons (PAHs) and soot, and heterogeneous reactions leading to the deposition of pyrolytic car-

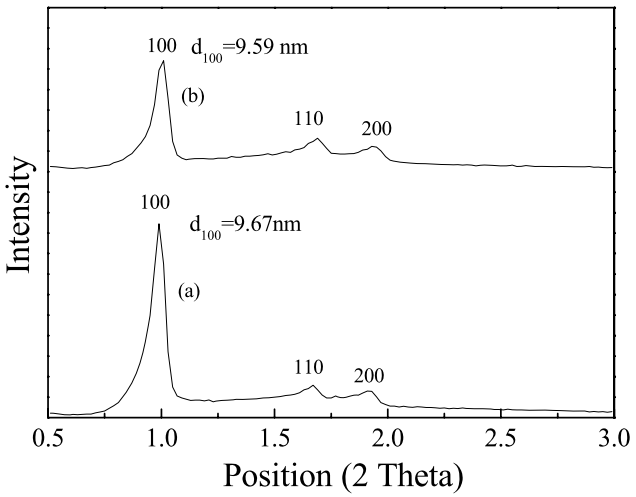

Fig. 3 XRD pattern of SBA-15 (**a**) before and (**b**) after heat treatment at 1073 K

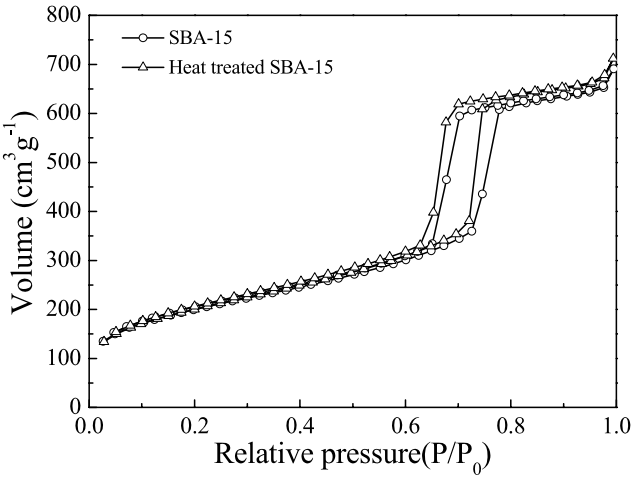

Fig. 4 N_2 adsorption isotherms of SBA-15 before and after heat treatment at 1073 K

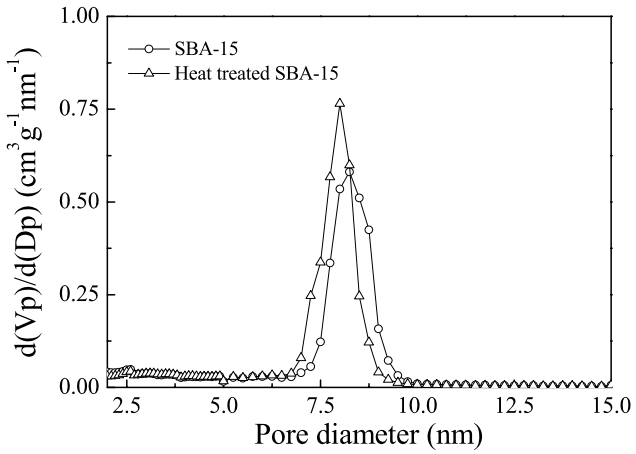

Fig. 5 DFT pore size distribution of SBA-15 before and after heat treatment at 1073 K

bon on the substrate surface. Therefore, the overall kinetics of the deposition process is determined by the kinetics of gas-phase and surface reactions and in particular the interaction or competition of gas-phase and surface reactions (Becker and Huttinger 1998; Prasetyo and Do 1999; Norinaga et al. 2006). CVD conditions (Becker and Huttinger 1998; Freitas and Figueiredo 2001) such as carbon deposition temperature, hydrocarbon type and concentration as well as residence time do have influence on the CVD process. Active sites may also be important for adsorption and surface reactions and hydrogen inhibition effect may also be involved (Benzinger et al. 1996). Based on previous studies, carbon pulse CVD on SBA-15 was conducted at high temperature of 1073 K, using acetylene as carbon precursor. Therefore, the thermal stability of the substrate is a prerequisite for the modification technique. Figure 3 shows the XRD pattern of SBA-15 before and after heat treatment at 1073 K.

As shown in Fig. 3, the small-angle XRD pattern of SBA-15 shows three well-resolved peaks indexable as (100), (110), (200) reflections, indicating a high degree of hexagonal mesoscopic organization. After heat treatment at 1073 K, SBA-15 still exhibits the typical XRD pattern of ordered hexagonal arrangement, indicating that the honeycomb-like structure can withstand such high temperature.

Figures 4 and 5 show the N_2 adsorption/desorption isotherms and DFT pore size distribution of SBA-15 before and after heat treatment at 1073 K, respectively. The structural properties of the two samples are summarized in Table 1. Consistent with the presence of uniform mesopores, the nitrogen adsorption-desorption isotherm of SBA-15 shows a type IV isotherm with clear type H1 (Zhao et al. 1998a, 1998b) hysteresis loop, which is a typical characteristic of mesoporous materials (see Fig. 4). Pore size distribution of SBA-15 calculated by the NLDFT method gives a narrow pore size distribution centered at around 8.1 nm. Micropore analysis based on t-plot method reveals that there is indeed a little amount of micropore existing in SBA-15, which exists on the pore wall of SBA-15 and is resulted from the mutually interpenetrating network of silica and hydrophilic EO chains formed during the assembly of the organic inorganic hybrid material (Shin et al. 2001). After heat treatment, as shown in Fig. 4, Fig. 5 and Table 1, there is little change in the shape of N_2 isotherm, BET specific surface area, total pore volume and pore size distribution, further confirming that the mesoporous structure did not collapse during the whole heating process. The little shift of the pore size distribution to smaller pores may be resulted from condensation of surface silanol groups at high temperature. The heat treatment experiment confirms that SBA-15 is thermally stable and suitable for carbon CVD modification although it results in partial elimination of micropores.

Table 1 Structural properties of SBA-15 before and after heat treatment at 1073 K

Sample	S_{BET} (m^2/g)	Total pore volume: V_{total} (cm^3/g)	Micropore volume: V_{micro} (cm^3/g)	Diameter of pore mouth: D_{mounth} (nm)
SBA-15	718	1.062	0.0396	8.1
Heat treated SBA-15	726	1.095	0.0268	8.1

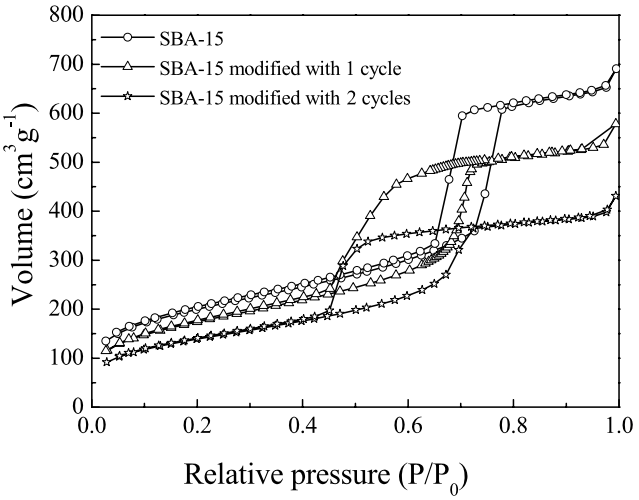

Fig. 6 N_2 adsorption isotherms of SBA-15 before and after modification with 1 and 2 cycles of carbon pulse CVD (C_2H_2 flow rate = 12 cm^3/min, N_2 flow rate = 48 cm^3/min, temperature = 1073 K, feeding time = 5 min)

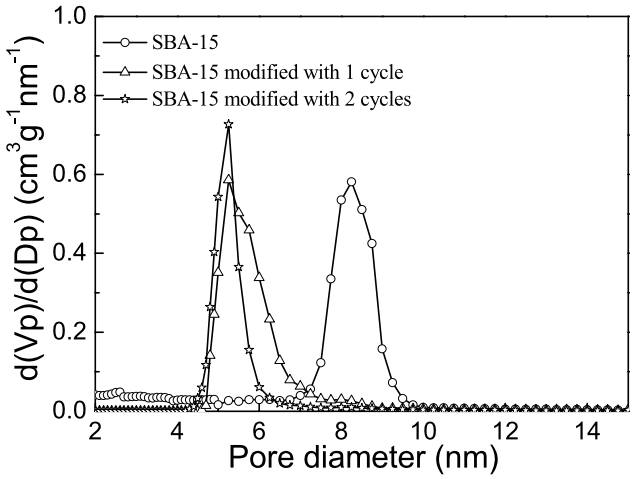

Fig. 7 DFT pore size distribution of SBA-15 before and after modification with 1 and 2 cycles of carbon pulse CVD (C_2H_2 flow rate = 12 cm^3/min, N_2 flow rate = 48 cm^3/min, temperature = 1073 K, feeding time = 5 min)

Figure 6 shows the N_2 adsorption isotherms of SBA-15 before and after modification with 1 and 2 cycles of carbon pulse CVD at temperature of 1073 K with a C_2H_2/N_2 ratio of 1/4, total flow rate of 60 cm^3/min and C_2H_2 feeding time of 5 min. The N_2 adsorption isotherms of the two modified samples both exhibit hysteresis loops indicating an ink-bottle-like pore structure. The hysteresis loops become enlarged after modification. The relative pressure indicating capillary condensation in mesopores is near to that of unmodified SBA-15, and the adsorption branch is almost parallel with that of unmodified SBA-15, indicating that there is little change in the pore body after modification. However, the desorption of N_2 molecules occurs at much lower relative pressure than that of unmodified SBA-15, indicating that desorption of N_2 molecules from the larger cavity is retarded by the smaller necks. For ink-bottle-like pores, desorption of N_2 occurs from the narrow neck and this is replenished from the larger parts of the pore (Do 1998).

The pore size distribution of the two modified SBA-15 samples is shown in Fig. 7, which further confirms that the pore mouth of SBA-15 has been reduced from 8.1 nm to 5.1 nm after the carbon pulse CVD process. However, the two modified SBA-15 samples with different number of cycles have nearly the same pore-opening size. No further decrease in pore-opening size is observed by increasing the number of cycles of carbon pulse CVD. Greater loss of BET specific surface area and adsorption capacity are observed by two runs of pulse CVD process. After one cycle of carbon pulse CVD, the BET surface area and pore volume is only reduced by 12% and 16%, respectively (see Table 2). However, after 2 cycles of carbon CVD, the loss of BET surface area and pore volume is increased to 30% and 38% (see Table 2). The reason why the second cycle of CVD cannot further reduce the pore opening of SBA-15 needs to be studied, but we suspect that polycyclic aromatic compounds, whose size is large than 5.1 nm, may be formed before carbon deposition.

In order to find out the optimal C_2H_2/N_2 ratio, SBA-15 was modified with different C_2H_2/N_2 ratios while keeping other parameters unchanged.

The N_2 adsorption isotherms of the samples modified with different C_2H_2/N_2 ratios (see Fig. 8) are plotted in Fig. 8. It is found that the sample modified with lower C_2H_2/N_2 ratio ($C_2H_2/N_2 = 1/9$) exhibits a relatively smaller hysteresis loop and the relative pressure indicating desorption occurrence is almost the same as that of unmodified SBA-15. Although the sample modified with higher C_2H_2/N_2 ratio ($C_2H_2/N_2 = 1/1$) gives a hysteresis loop indicating an ink-bottle-like pore structure, the adsorption capacity was much lower than that of the sample modified

Table 2 Structural properties of SBA-15 before and after modification with 1 and 2 cycles of carbon pulse CVD

Sample	S_{BET} (m^2/g)	V_{total} (cm^3/g)	D_{mouth} (nm)
SBA-15	718	1.062	8.1
SBA-15 modified with 1 cycle	632	0.888	5.1
SBA-15 modified with 2 cycles	505	0.663	5.1

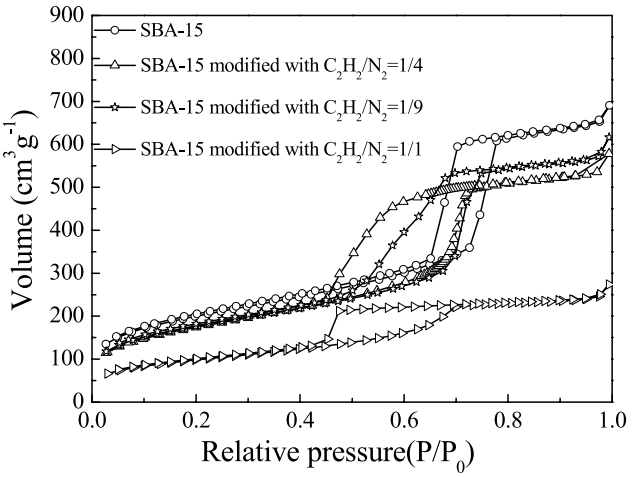

Fig. 8 N_2 adsorption isotherms of SBA-15 before and after modification using different C_2H_2/N_2 ratios (1 cycle of pulse CVD, total flow rate = 60 cm^3/min, temperature = 1073 K, feeding time = 5 min)

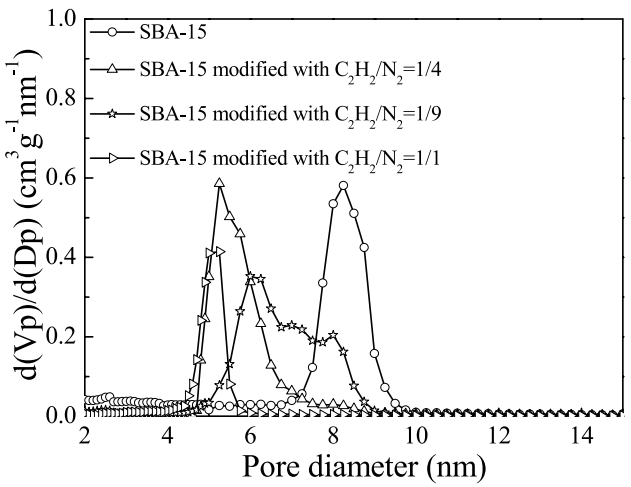

Fig. 9 DFT pore size distribution of SBA-15 before and after modification using different C_2H_2/N_2 ratios (1 cycle of pulse CVD, total flow rate = 60 cm^3/min, temperature = 1073 K, feeding time = 5 min)

with C_2H_2/N_2 ratio of 1/4. This is so because too much carbon was deposited onto SBA-15 at such a high C_2H_2/N_2 ratio of 1/1.

The pore size distributions of the three samples modified with different C_2H_2/N_2 ratios are shown in Fig. 9. It is seen that the sample modified with lower C_2H_2/N_2 ratio ($C_2H_2/N_2 = 1/9$) exhibits a very broad pore size distribution. It means that this C_2H_2 concentration is too low to uniformly deposit carbon on the substrate in such a short period of time. The pore opening size of the sample modified with higher C_2H_2/N_2 ratio ($C_2H_2/N_2 = 1/1$) is the same as the sample modified with C_2H_2/N_2 ratio of 1/4. However, the peak intensity is much lower. No further decrease in the pore-opening size is observed using higher C_2H_2/N_2 ratio. Moreover, higher C_2H_2/N_2 ratio also results in greater loss of BET specific surface area and total pore volume. The loss of the BET specific surface area and total pore volume is increased to 51% and 60% (see Table 2) when using a C_2H_2/N_2 ratio of 1/1.

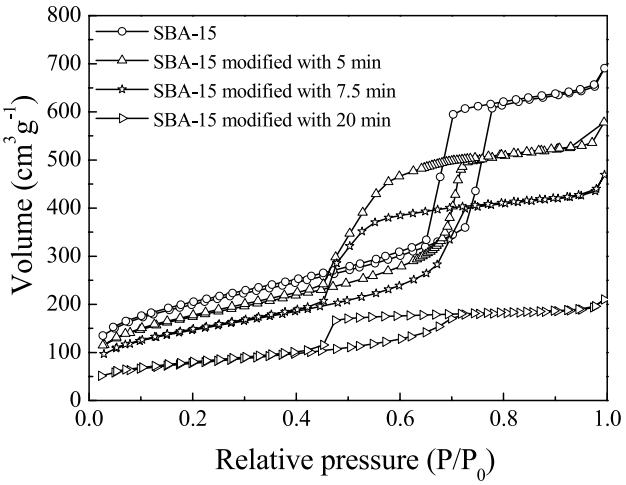

Fig. 10 N_2 adsorption isotherms of SBA-15 before and after modification using different C_2H_2 feeding time (1 cycle of pulse CVD, C_2H_2 flow rate = 12 cm^3/min, N_2 flow rate = 48 cm^3/min, temperature = 1073 K)

To investigate the influence of C_2H_2 feeding time on the carbon deposition process, longer C_2H_2 feeding time was tried while keeping other parameters unchanged.

As shown in Fig. 10, the two samples modified with longer feeding time both exhibit hysteresis loops characteristic of ink-bottle-like pore structure. However, the adsorption capacity decreases with increasing C_2H_2 feeding time, suggesting that longer feeding time cannot further reduce the pore opening size but simply deposit more carbon on the external surface of SBA-15.

The pore size distributions of the three samples modified with different C_2H_2 feeding time are plotted in Fig. 11, which shows that the two samples modified with longer

Table 3 Structural properties of SBA-15 before and after modification using different C_2H_2/N_2 ratios

Sample	S_{BET} (m^2/g)	V_{total} (cm^3/g)	D_{mouth} (nm)
SBA-15	718	1.062	8.1
SBA-15 modified with $C_2H_2/N_2 = 1/4$	632	0.888	5.1
SBA-15 modified with $C_2H_2/N_2 = 1/9$	640	0.948	6.1
SBA-15 modified with $C_2H_2/N_2 = 1/1$	355	0.420	5.1

Table 4 Structural properties of SBA-15 before and after modification using different C_2H_2 feeding time

Sample	S_{BET} (m^2/g)	V_{total} (cm^3/g)	D_{mouth} (nm)
SBA-15	718	1.062	8.1
SBA-15 modified with 5 min	632	0.888	5.1
SBA-15 modified with 7.5 min	533	0.721	5.1
SBA-15 modified with 20 min	279	0.323	5.1

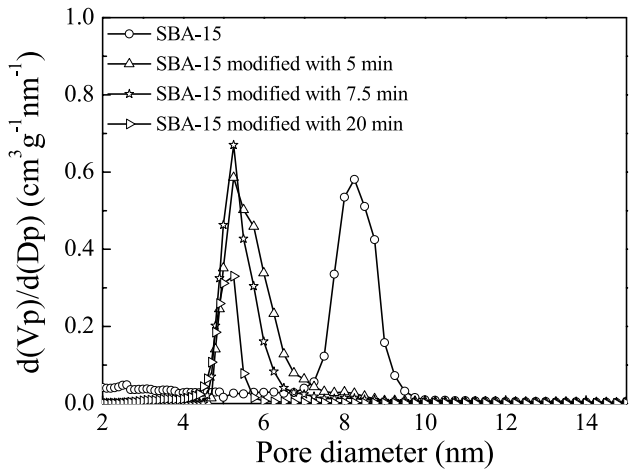

Fig. 11 DFT pore size distribution of SBA-15 before and after modification using different C_2H_2 feeding time (1 cycle of pulse CVD, C_2H_2 flow rate = 12 cm^3/min, N_2 flow rate = 48 cm^3/min, temperature = 1073 K)

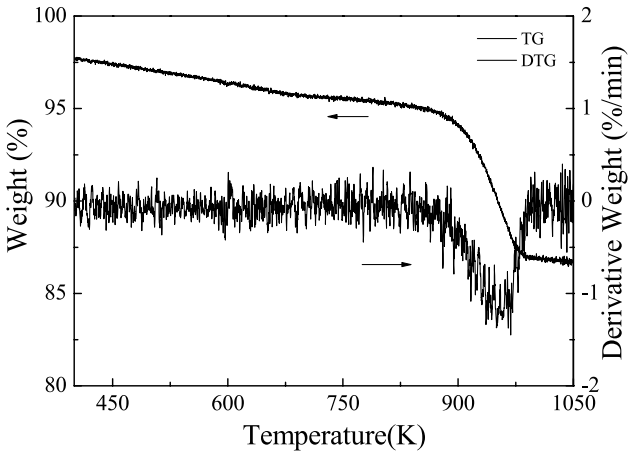

Fig. 12 TG and DTG curves of Ink-bottle-like SBA-15/carbon composite

C_2H_2 feeding time have the same pore-opening size as that of the sample modified with 5 min. However, the loss of BET surface area and total pore volume increases significantly with C_2H_2 feeding time increases (26% and 32% for the sample modified with 7.5 min and 61% and 70% for the sample modified with 20 min, respectively), indicating that 5 min C_2H_2 feeding time is long enough to modify the pore opening size.

By using C_2H_2 as the carbon precursor, it is found that the pore-mouth of SBA-15 can be effectively reduced from 8.1 nm to 5.1 nm in a very short period of time. Surprisingly, further decrease in the pore-opening size cannot be achieved by using more number of cycles of pulse CVD or higher C_2H_2/N_2 ratio or longer C_2H_2 feeding time, which can only result in further loss of BET specific surface area and total pore volume. This may be explained by the polymerization phenomena during C_2H_2 cracking process. C_2H_2 is very active at the temperature of 1073 K and could form large aromatic hydrocarbons with molecular diameter larger than 5.1 nm. Therefore, it is possible that, when the pore mouth decreases to 5.1 nm, the large aromatic hydrocarbon molecules could not enter the pore and preferentially deposit on the external surface, resulting in further decrease of BET specific surface area and total pore volume while the pore-mouth diameter remains unchanged.

To investigate the influence of the carbon pulse CVD process on particle morphology and periodic pore arrangement, the ink-bottle-structured SBA-15/carbon composite (modified under the experiment condition of 1 cycle of pulse CVD, C_2H_2 flow rate of 12 cm^3/min, N_2 flow rate of 48 cm^3/min, CVD temperature of 1073 K, C_2H_2 feeding time of 5 min) was further characterized with TGA, SEM, XRD and TEM techniques.

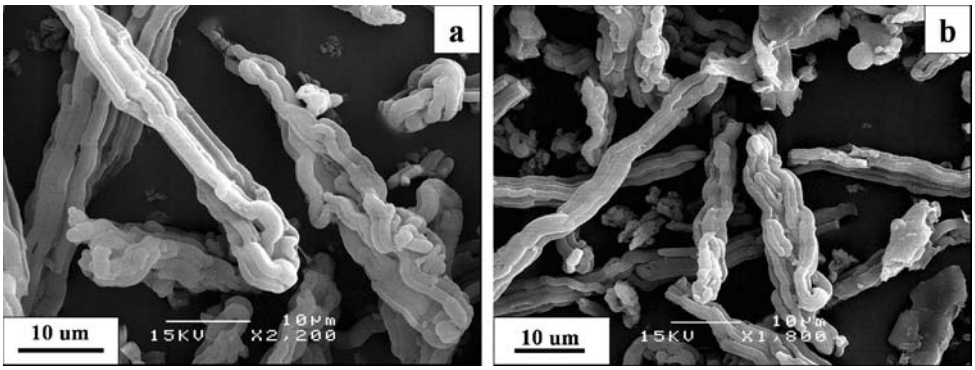

Fig. 13 SEM images of (**a**) SBA-15 and (**b**) ink-bottle-like SBA-15/carbon composite

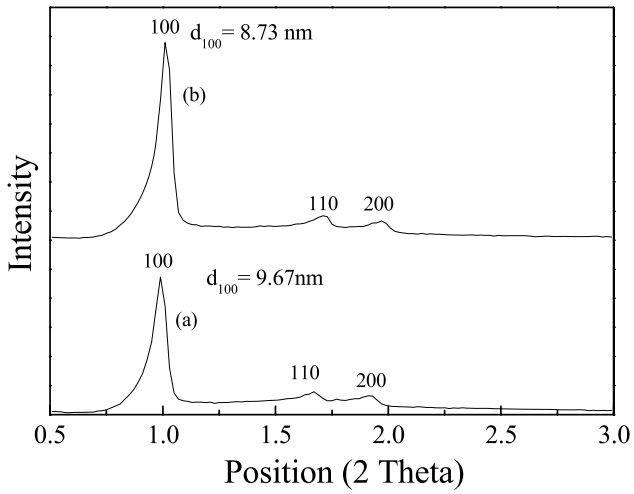

Fig. 14 XRD patterns of (**a**) SBA-15 and (**b**) ink-bottle-like SBA-15/carbon composite

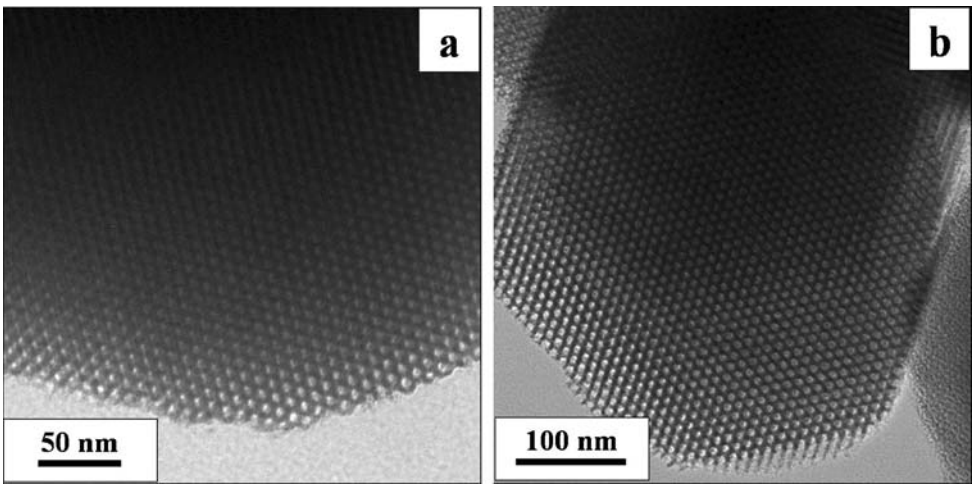

Fig. 15 TEM images of (**a**) SBA-15 and (**b**) ink-bottle-like SBA-15/carbon composite

Figure 12 shows the weight loss profile and derivative weight change curve of the ink-bottle-like pore structured SBA-15/carbon composite. The intense weight loss between 873 K and 1020 K can be attributed to the burning of carbon upon heating, which indicates that the composite contains about 8.7 wt% of carbon. The SEM images shown in Fig. 13 reveal that the composite retains the particle morphology of SBA-15, consisting of many uniform rope-like domains. Three resolved diffraction peaks (100), (110) and (200) are also observed in the XRD pattern of the composite as illustrated in Fig. 14, indicating that the ink-bottle-like SBA-15/carbon composite still exhibits highly ordered hexagonal structure. The retention of hexagonal ordered pore structure is further confirmed by the TEM image of SBA-15 and the composite (see Fig. 15).

4 Conclusions

In conclusion, carbon pulse CVD is a novel, easy and feasible method to modify the pore opening of SBA-15. By finely choosing the CVD conditions, ink-bottle-like pore structured SBA-15/carbon composite with pore mouth diameter of 5.1 nm, pore body diameter of 8.1 nm, high BET specific surface area (632 m^2/g) and large pore volume (0.888 cm^3/g) can be successfully synthesized. The SBA-15/carbon composite is highly hexagonally ordered and has similar particle morphology to that of SBA-15. The formation of large aromatic hydrocarbons with molecular diameter larger than 5.1 nm during C_2H_2 cracking hinders the further reduction in the pore-opening size of SBA-15. Other carbon precursor may be studied in order to further reduce the pore-opening size.

Acknowledgement Financial support from the Research Grants Council of Hong Kong (CERG, Project No.617305) is gratefully acknowledged.

References

Becker, A., Huttinger, K.J.: Chemistry and kinetics of chemical vapor deposition of pyrocarbon. II. Pyrocarbon deposition from ethylene, acetylene and 1,3-butadiene in the low temperature regime. Carbon **36**, 177–199 (1998)

Begum, H.A., Katada, N., Niwa, M.: Chemical vapor deposition of silica on silicalite crystals and shape-selective adsorption of paraffins. Microporous Mesoporous Mater. **46**, 13–21 (2001)

Benzinger, W., Becker, A., Huttinger, K.J.: Chemistry and kinetics of chemical vapor deposition of pyrocarbon. I. Fundamentals of kinetics and chemical reaction engineering. Carbon **34**, 957–966 (1996)

Carrott, R., Cansado, I.P.P., Carrott, M.M.L.R.: Carbon molecular sieves from PET for separations involving CH_4, CO_2, O_2 and N_2. Appl. Surf. Sci. **252**, 5948–5952 (2006)

Choi, M., Heo, W., Kleitz, F., Ryoo, R.: Facile synthesis of high quality mesoporous SBA-15 with enhanced control of the porous network connectivity and wall thickness, Chem. Commun., 1340–1341 (2003)

David, E., Talaie, A., Stanciu, V., Nicolae, A.C.: Synthesis of carbon molecular sieves by benzene pyrolysis over microporous carbon materials. J. Mater. Process. Technol. **157–158**, 290–296 (2004)

de la Casa-Lillo, M.A., Moore, B.C., Cazorla-Amoros, D., Linares-Solano, A.: Molecular sieve properties obtained by cracking of methane on activated carbon fibers. Carbon **40**, 2489–2494 (2002)

Do, D.D.: Adsorption Analysis: Equilibria and Kinetics, pp. 142–143, Imperial College Press, London (1998)

Fodor, K., Bitter, J.H., de Jong, K.P.: Investigation of vapor-phase silica deposition on MCM-41, using tetraalkoxysilanes. Microporous Mesoporous Mater. **56**, 101–109 (2002)

Freitas, M.M.A., Figueiredo, J.L.: Preparation of carbon molecular sieves for gas separations by modification of the pore sizes of activated carbons. Fuel **80**, 1–6 (2001)

Hibino, T., Niwa, M., Murakami, Y.: Shape-selectivity over HZSM-5 modified by chemical vapor-deposition of silicon. J. Catal. **128**, 551–558 (1991)

Hu, X., Qiao, S., Zhao, X.S., Lu, G.Q.: Adsorption study of benzene in ink-bottle-like MCM-41. Ind. Eng. Chem. Res. **40**, 862–867 (2001)

Kawabuchi, Y., Kishino, M., Kawano, S., Whitehurst, D.D., Mochida, I.: Carbon deposition from benzene and cyclohexane onto active carbon fiber to control its pore size. Langmuir **12**, 4281–4285 (1996)

Kawabuchi, Y., Sotowa, C., Kishino, M., Kawano, S., Whitehurst, D.D., Mochida, I.: Chemical vapor deposition of heterocyclic compounds over active carbon fiber to control its porosity and surface function. Langmuir **13**, 2314–2317 (1997)

Kruk, M., Jaroniec, M., Joo, S.H., Ryoo, R.: Characterization of regular and plugged SBA-15 silica by using adsorption and inverse carbon replication and explanation of the plug formation mechanism. J. Phys. Chem. B **107**, 2205–2213 (2003)

Kunkeler, P.J., Moeskops, D., vanBekkum, H.: Zeolite beta: characterization and passivation of the external surface acidity. Microporous Mater. **11**, 313–323 (1997)

Mehn, D., Konya, Z., Halasz, J., Nagy, J.B., Rac, B., Molnar, A., Kiricsi, I.: Flexibility of the MCM-41 structure: pore expansion and wall-thickening in MCM-41 derivatives. Appl. Catal. A **232**, 67–76 (2002)

Norinaga, K., Deutschmann, O., Huttinger, K.J.: Analysis of gas phase compounds in chemical vapor deposition of carbon from light hydrocarbons. Carbon **44**, 1790–1800 (2006)

Paredes, J.I., Villar-Rodil, S., Martinez-Alonso, A., Tascon, J.M.D.: A scanning tunnelling microscopy insight into the preparation of carbon molecular sieves by chemical vapour deposition. J. Mater. Chem. **13**, 1513–1516 (2003)

Prasetyo, I., Do, D.D.: Pore structure alteration of porous carbon by catalytic coke deposition. Carbon **37**, 1909–1918 (1999)

Shin, H.J., Ryoo, R., Kruk, M., Jaroniec, M.: Modification of SBA-15 pore connectivity by high-temperature calcination investigated by carbon inverse replication, Chem. Commun., 349–350 (2001)

Villar-Rodil, S., Martinez-Alonso, A., Tascon, J.M.D.: Carbon molecular sieves for air separation from Nomex aramid fibers. J. Colloid Interface Sci. **254**, 414–416 (2002)

Villar-Rodil, S., Martinez-Alonso, A., Pajares, J.A., Tascon, J.M.D., Jasienko-Halat, M., Broniek, E., Kaczmarczyk, J., Jankowska, A., Albiniak, A., Siemieniewska, T.: Following changes in the porous texture of Nomex-derived activated carbon fibres with the molecular probe technique. Microporous Mesoporous Mater. **64**, 11–19 (2003)

Villar-Rodil, S., Navarrete, R., Denoyel, R., Albiniak, A., ParedesI, J.I., Martinez-Alonso, A., Tascon, J.M.D.: Carbon molecular sieve cloths prepared by chemical vapour deposition of methane for separation of gas mixtures. Microporous Mesoporous Mater. **77**, 109–118 (2005)

Weber, R.W., Moller, K.P., Unger, M., O'Connor, C.T.: The chemical vapour and liquid deposition of tetraethoxysilane on the external surface of ZSM-5. Microporous Mesoporous Mater. **23**, 179–187 (1998)

Weber, R.W., Moller, K.P., O'Connor, C.T.: The chemical vapour and liquid deposition of tetraethoxysilane on ZSM-5, mordenite and beta. Microporous Mesoporous Mater. **35–6**, 533–543 (2000)

Yue, Y.H., Tang, Y., Liu, Y., Gao, Z.: Chemical liquid deposition zeolites with controlled pore-opening size and shape-selective separation of isomers. Ind. Eng. Chem. Res. **35**, 430–433 (1996)

Yue, Y.H., Tang, Y., Gao, Z.: Zeolite pore size engineering by chemical liquid deposition. Stud. Surf. Sci. Catal. **105**, 2059–2065 (1997)

Zhao, X.S.: Synthesis, modification, characterization and application of MCM-41 for VOC control, Thesis (Ph.D.), pp. 37–39, University of Queensland, Brisbane (1998)

Zhao, D.Y., Feng, J.L., Huo, Q.S., Melosh, N., Fredrickson, G.H., Chmelka, B.F., Stucky, G.D.: Triblock copolymer syntheses of mesoporous silica with periodic 50–300 Angstrom pores. Science **279**, 548–552 (1998a)

Zhao, D.Y., Huo, Q.S., Feng, J.L., Chmelka, B.F., Stucky, G.D.: Nonionic triblock and star diblock copolymer and oligomeric surfactant syntheses of highly ordered, hydrothermally stable, mesoporous silica structures. J. Am. Chem. Soc. **120**, 6024–6036 (1998b)

Zhao, X.S., Lu, G.Q.M., Hu, X.: A novel method for tailoring the pore-opening size of MCM-41 materials, Chem. Commun., 1391–1392, (1999)

Zheng, S.R., Heydenrych, H.R., Jentys, A., Lercher, J.A.: Influence of surface modification on the acid site distribution of HZSM-5. J. Phys. Chem. B **106**, 9552–9558 (2002)